Front propagation in an $A \to 2A$, $A \to 3A$ process in one dimension: Velocity, diffusion, and velocity correlations

Niraj Kumar,[1,*] Goutam Tripathy,[1] and Katja Lindenberg[2]
[1]*Institute of Physics, Sachivalaya Marg, Bhubaneswar 751005, India*
[2]*Department of Chemistry and Biochemistry, and BioCircuits Institute, University of California San Diego, La Jolla, California 92093-0340, USA*

(Received 1 February 2011; revised manuscript received 31 March 2011; published 29 June 2011)

We study front propagation in the reaction-diffusion process $\{A \xrightarrow{\epsilon} 2A, A \xrightarrow{\epsilon_t} 3A\}$ on a one-dimensional lattice with hard-core interactions between the particles. Using the leading particle picture, the velocity of the front is computed using different approximate methods that yield results in good agreement with simulation results. We observe that the front dynamics exhibits temporal velocity correlations that must be accounted for to obtain accurate estimates of the front diffusion coefficient. Interestingly, these temporal correlations change sign depending upon the sign of $\epsilon_t - D$, where D is the bare diffusion coefficient of A particles. For $\epsilon_t = D$, we find analytically as well as numerically that the leading particle and thus the front move as an uncorrelated random walker.

DOI: 10.1103/PhysRevE.83.061152 PACS number(s): 05.40.−a

I. INTRODUCTION

Fronts that separate different phases occur in a large number of physical, chemical, and biological settings [1–4]. The propagation of such fronts is a ubiquitous phenomenon when such systems are away from equilibrium. In this paper we study the front dynamics in the reaction-diffusion system $A \xrightarrow{\epsilon} 2A$, $A \xrightarrow{\epsilon_t} 3A$ in a one-dimensional (1D) lattice. The front separates a region asymptotically fully occupied by A particles from a region that is asymptotically empty. Hard-core interactions between particles are enforced by allowing each lattice site to be empty or occupied by at most one particle. The unique feature of our model lies in the occurrence of the "twin" creation process $A \to 3A$, in addition to the more familiar single creation process $A \to 2A$. The twin creation process along with the hard-core interactions leads to interesting *temporal* velocity correlations. These temporal correlations, and our ability to provide analytic results, motivate this work.

A mean-field description of the model is provided by the partial differential equation for the coarse grained concentration $\rho(x,t)$,

$$\frac{\partial \rho}{\partial t} = \Gamma \frac{\partial^2 \rho}{\partial x^2} + a\rho - b\rho^2 + c\rho^3, \tag{1}$$

where Γ is an effective diffusion coefficient [5], and a, b, and c are related to the two microscopic processes of rate ϵ and ϵ_t of particle creation. This description is expected to hold at the macroscopic level.

Equation (1) reduces to the well-known Fisher equation [6] in the absence of the twin creation process $A \to 3A$. The front dynamics in the microscopic lattice model for $A \to 2A$ using two-site correlations has been studied extensively [7–12]. The inclusion of the process $A \to 3A$ involves three-site correlations and gives rise to interesting results as reported in this paper.

The mean-field description admits traveling-wave solutions of the form $\rho(x,t) = \phi(x - vt)$, where the velocity of an initially sharp front between the $\rho = 1$ (stable) and $\rho = 0$ (unstable) states approaches an asymptotic velocity $V_0 = 2\sqrt{a\Gamma}$. The important feature to be noted here is that a mean-field equation fails to deal with internal fluctuations arising from the discrete nature of the reacting species, especially in lower dimensions or when, as in our case, the occupancy per site is small. As shown for the diffusion-controlled process $2A \to 0$, the mean-field theory predicts a decay of the global concentration $\rho(t) = \int dx\, \rho(x,t)$ that goes asymptotically as $\rho(t) \sim 1/t$. However, in lower dimensions it has been observed that the decay of $\rho(t)$ is slower than $1/t$. In fact, in 1D, $\rho(t) \sim t^{-1/2}$ while in 2D, $\rho(t) \sim \ln t/t$ [13]. Similarly, for the front dynamics in $A \leftrightarrow 2A$, it is known that even for very large occupancy N per site behind the front, discreteness effects always affect the front, and the front velocity V converges very slowly to the mean-field velocity $|V - V_0| \sim 1/\ln^2 N$ [14]. The mean-field results are recovered for $N \to \infty$. Thus, for macroscopic systems one can safely neglect these correlations. However, for systems with a finite number of particles and/or in lower dimensions, fluctuation-induced behavior emerges [15,16].

We focus on a 1D lattice and, using a leading particle picture, we study the front velocity and the diffusion coefficient. We find analytic estimates for the front velocity using different approximate methods which are in increasingly good agreement with Monte Carlo simulation results. Accounting for temporal correlations is not necessary to obtain these accurate results. However, we find that an accurate calculation of the front diffusion coefficient requires that one take into account temporal velocity correlations. Interestingly, it is observed that these correlations change sign depending on the sign of $c - \Gamma$. For $c = \Gamma$, we find analytically as well as numerically that the leading particle and thus the front move as an uncorrelated random walker. For this special case, through an explicit analysis, we show that two successive steps are uncorrelated.

*Present address: Department of Chemistry and Biochemistry, and BioCircuits Institute, University of California San Diego, La Jolla, CA 92093-0340.

II. MODEL

We consider a 1D lattice of sites i and start with a step function-like distribution where the left half ($i \leqslant 0$) is filled with A particles while the right half ($i > 0$) is empty. The size L of the lattice is chosen to be sufficiently large for boundaries not to be of concern. We update the system random sequentially, with L microscopic moves corresponding to one Monte Carlo step (MCS). Explicitly, each update consists of the random selection of a site with uniform probability from among the L sites of the lattice. If the chosen site is occupied, then the particle at that site can undergo one of three microscopic moves: (1) It can jump to the left or right nearest-neighbor site if it is empty, i.e., (10) $\rightarrow$ (01) (right jump) or (01) $\rightarrow$ (10) (left jump), each with rate D. Here (10) corresponds to a configuration of a pair of neighboring sites, with 1 and 0 representing occupied and empty sites, respectively. (2) The particle can give birth to one particle at the left or right nearest-neighboring site if that site is empty, i.e., (10) $\rightarrow$ (11) or (01) $\rightarrow$ (11), each with rate ϵ. (3) The particle can generate two new particles at both the neighboring sites provided *both* are empty, i.e., (010) $\rightarrow$ (111) with rate ϵ_t. These choices of microscopic moves lead to the following values for the parameters in Eq. (1): $a = 2\epsilon + \epsilon_t$, $b = 2\epsilon + 2\epsilon_t$, $c = \epsilon_t$, and $\Gamma = D$.

As time evolves, these microscopic moves result in the stochastic motion of the front which may be identified with the leading A particle. After a transient time, the front reaches an asymptotic state and we wish to compute the speed and diffusion coefficient of the front in this regime. Let us denote by $P(X,t)$, the probability of finding the leading A particle at X at time t, and by $Q_0(X,t)$, the joint probability of finding the leading particle at X *and* the site immediately to the left of it to be empty. Then the equation for the evolution of $P(X,t)$ is [17–19]

$$\begin{aligned}\frac{\partial P(X,t)}{\partial t} &= (\epsilon + D)P(X-1,t) + \epsilon_t Q_0(X-1,t) \\ &\quad + D Q_0(X+1,t) - (\epsilon + D)P(X,t) \\ &\quad - (\epsilon_t + D)Q_0(X,t). \end{aligned} \tag{2}$$

This is not a closed equation for $P(X,t)$ because $Q_0(X,t)$ is also unknown at this point. The latter joint probability can in turn be written as

$$Q_0(X,t) = [1 - \rho(X-1,t)]\, P(X,t), \tag{3}$$

where $\rho(X-1,t)$ is the conditional probability that site $X-1$ is occupied given that the front is at X at time t. This conditional probability is also unknown at this point. In fact, to determine the evolution of Q_0 requires the introduction of an infinite hierarchy of such conditional probabilities involving sites further and further removed from the front. We will not do this but instead will introduce appropriate approximations when needed.

The speed V and the diffusion coefficient D_f of the front are in general defined as

$$V = \lim_{t\to\infty} \frac{d}{dt}\langle X(t)\rangle, \tag{4}$$

$$D_f = \frac{1}{2}\lim_{t\to\infty} \frac{d}{dt}[\langle (X^2(t)\rangle - \langle X(t)\rangle^2], \tag{5}$$

where $\langle f(X,t)\rangle \equiv \sum_X f(X,t)P(X,t)$. Note that D and D_f differ because the former is a microscopic rate of motion to a site given that it is empty, while D_f is a macroscopic diffusion coefficient that includes the occupancy information. We write

$$\rho_1(t) \equiv \sum_X \rho(X-1,t)P(X,t). \tag{6}$$

This is the probability that the site behind the leading particle is occupied at time t. Using the normalization $\sum_X P(X) = 1$ along with the time-independent limit $\rho_1(t) \rightarrow \rho_1$ in the steady state, we arrive at the expression for the asymptotic velocity of the front,

$$V = \epsilon + \epsilon_t - \rho_1(\epsilon_t - D). \tag{7}$$

The only unknown in this expression, which is exact, is ρ_1. The diffusion coefficient is given from Eq. (5) as

$$\begin{aligned} D_f &= \frac{1}{2}\{\epsilon + \epsilon_t + 2D - \rho_1(\epsilon_t + D)\} \\ &\quad + (\epsilon_t - D)\left[\sum_X X Q_0(X) - (1-\rho_1)\sum_X X P(X)\right]. \end{aligned} \tag{8}$$

This quantity requires knowledge of the full evolution of the system. However, if we implement the approximation $\rho(X-1,t) \rightarrow \rho_1$, that is, that in the steady state the conditional probability can be approximated by the density at the site behind the leading particle, then the second line drops out and we arrive at the approximate expression

$$D_0 = \frac{1}{2}\{\epsilon + \epsilon_t + 2D - \rho_1(\epsilon_t + D)\}. \tag{9}$$

We have replaced the subscript f on D by a 0 to stress that an approximation has been made. In this expression once again the only unknown is ρ_1. At this point we do not know the severity of this approximation, whose effect is to neglect temporal correlations implicit in Eq. (2). In an interacting system, we cannot *a priori* neglect such correlations. It now remains to determine the unknown steady-state density ρ_1 behind the front, and to assess the severity of the approximation.

Expressions (7) and (9) for the front velocity and diffusion coefficient can be understood by visualizing the front as a random walker that moves to the left or right with certain rates. For such a walker, the velocity and diffusion coefficient are given as $R_r - R_l$ and $(R_r + R_l)/2$, respectively, where R_r and R_l are the rates at which the walker moves to the right or left. In our model the front moves to the left with rate $R_l = D(1-\rho_1)$, which corresponds to hopping of the front to the left site if it is empty. To find the rate with which the front moves to the right, we first note that this can happen in three ways. It can happen if the front either jumps or gives birth to a single particle at the right empty site, or if it generates two particles at the neighboring sites, provided the site just behind it is empty, i.e., $R_r = D + \epsilon + \epsilon_t(1-\rho_1)$. Using these rates one can find the front velocity and diffusion coefficient as given by Eqs. (7) and (9), respectively. Here it is important to note

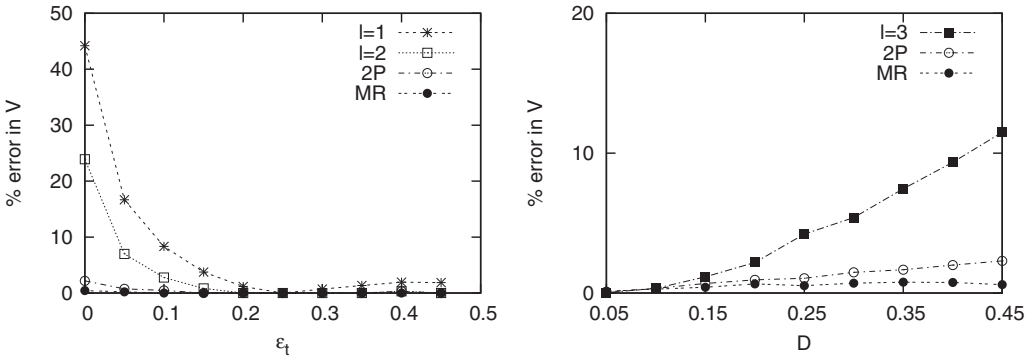

FIG. 1. (a) Percentage relative error in V, i.e., $(|V^s - V^a|/V^s) \times 100$ (V^s and V^a representing simulation and analytic results, respectively), vs ϵ_t, with $D = 0.25$ and $\epsilon = 0.025$. $l = 1$ (stars), $l = 2$ (open squares), 2P (open circles), and MR (filled circles). The simulation and analytic profile using MR are almost coincident for the range of parameters explored. (b) Percentage relative error in V vs D, with $\epsilon = 0.05$ and $\epsilon_t = 0$. The top data (filled squares) corresponds to Ref. [7] for $l = 3$ (eight states). The middle data (open circles) corresponds to the Kerstein [11] two-particle self-consistent representation, while the bottom data (filled circles) is the result of the mixed representation.

that the master equation (2) with the approximation discussed above is based on the assumption that the future evolution of the system is sensitive only to the present state of the system and thus describes a simple random walk which neglects temporal correlations in subsequent steps [20]. However, as we will see later, this is in general not the case; indeed, we will see that the front here moves as a *correlated* random walker. Thus we interpret D_0 as the front diffusion coefficient in the absence of any temporal correlations, and will subsequently find corrections to this expression.

We note that Eqs. (7) and (8) are exact, and that the static correlations in the problem are embodied in the quantity ρ_1. In Ref. [9], where $\epsilon_t = 0$, it was shown that the front velocity asymptotically approaches the mean-field value $V = V_0 = 2\sqrt{2\epsilon D}$ in the limit $D/\epsilon \to \infty$, while $V = \epsilon + D \sim \epsilon$ in the opposite limit $D/\epsilon \to 0$. However, between these two extreme limits we need to know ρ_1, and we expect to require knowledge of ρ_1 for $\epsilon_t \neq 0$.

Before proceeding to compute ρ_1 for the most general case, we discuss some special cases. (i) For $D = 0$, no vacancies can be created between two A particles and thus the asymptotic front profile is a sharp step. Consequently, no twin production takes place (as the site to the left of the leading particle is always occupied, that is, $\rho_1 = 1$). Hence the speed should be independent of ϵ_t, as confirmed from Eq. (7): $V = \epsilon$. In this limit Eq. (9) gives $D_0 \simeq \epsilon/2$. (ii) For $D = \epsilon_t$, one obtains $V = \epsilon + \epsilon_t$ independently of ρ_1. More interestingly, in this case $D_f = D_0$, i.e., the front moves as an uncorrelated random walker.

III. FRONT VELOCITY

In this section we present three approximate analytic methods to estimate ρ_1 and with this the front velocity as obtained given in Eq. (7). The first method is the so-called *fixed site representation* discussed in Ref. [7]. In this method, a truncated master equation is written in the frame moving with the front to describe the evolution of particles up to a given number (l) of sites behind the front. The density at the $(l+1)$st site behind the front is approximated as the bulk density, i.e., $\rho_{l+1} = 1$. In Appendix A we have illustrated this scheme for $l = 1$. In this case we work with a set of two states, {01} and {11}, with the rightmost "1" representing the front particle and a "0" representing an empty site. As shown in Fig. 1, the front velocity V estimated with this approximation is in reasonable agreement with the simulation results. For the special case $D = \epsilon_t$, as discussed earlier, the figure confirms that the theoretical result agrees *exactly* with the simulation result. We also notice that the approximate analytic results in general show improved agreement with the simulation results for larger values of ϵ_t. Conversely, as ϵ_t decreases and approaches zero, we see a gradual departure of the simulation data from the analytic outcome. This is due to the fact that the density at the ith site behind the front, ρ_i, differs significantly from the bulk density as ϵ_t decreases. This is shown in Fig. 2. The estimate for the velocity can be further improved if we explicitly include a larger number of sites in the dynamical description, that is, if we increase l. For example, for $l = 2$ we consider the explicit evolution of four states: {001}, {011}, {101}, and {111}. The improved results are shown in Fig. 1.

The second approximate method is the *two-particle representation* (2P) proposed by Kerstein [11]. Here each state

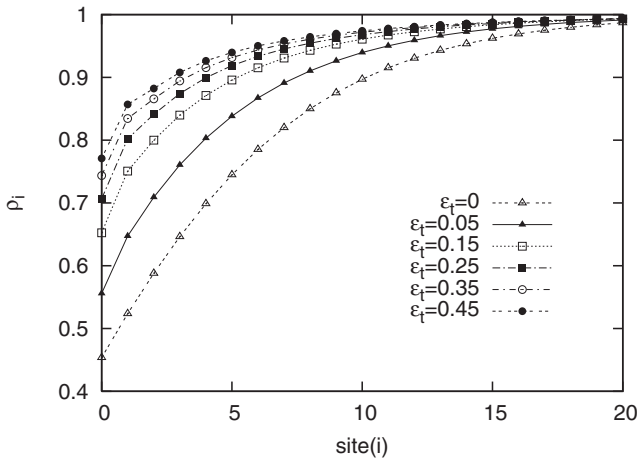

FIG. 2. Density profile behind the front for different values of ϵ_t, for $D = 0.25$ and $\epsilon = 0.025$. As ϵ_t decreases, the density profile curve shifts away from the bulk density level.

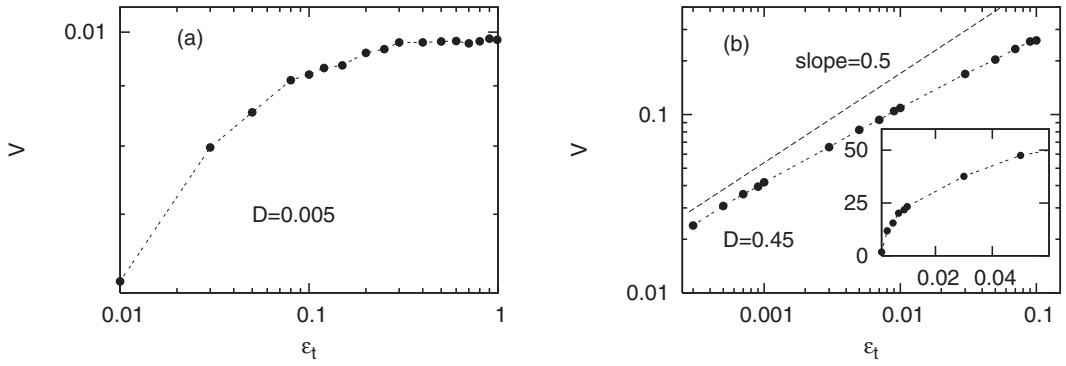

FIG. 3. Front velocity V vs ϵ_t for $\epsilon = 0$ and two different values of D on a log-log scale. In (a) we vary ϵ_t from 0.01 to 0.99 while in (b) we vary ϵ_t from 0.003 to 0.10. The inset in (b) plots the percentage relative difference $(|V - V_0|/V) \times 100$ as a function of ϵ_t. V_0 is the mean-field prediction.

of the system is defined by only the two rightmost particles. This leads to an infinite set of states: {11}, {101}, {1001}, {10001}, {100001}, ... The rightmost "1" represents the front particle and the leftmost "1" the second particle. We have computed ρ_1 using this scheme for the process under study (see Appendix B). The results obtained using this method are in good agreement with the simulation results marked 2P in Fig. 1.

Since we are dealing with a multiparticle interacting system, it is in general desirable to include a larger number of particles in the explicit state to find better analytic estimates. Motivated by this, we propose a scheme, which we call the *mixed representation*, in which we explicitly include all states that have either two or three particles. Thus, the set of states that we study here is {011}, {111}, {0101}, {1101}, . . ., and obtain an estimate for ρ_1 using a procedure similar to that used in the 2P representation (see Appendix C). This representation can be considered as the simplest extension of two-particle representations and yields better results than either of the above two schemes. The results are marked as MR in Fig. 1.

Finally, we have also studied the front dynamics in two interesting limits, namely, diffusion-controlled and reaction-controlled dynamics. In the diffusion-controlled limit, $D \ll \epsilon_t \sim \epsilon$, we expect the front velocity to be independent of ϵ_t, which is confirmed by our simulation results [Fig. 3(a)]. In the reaction-controlled limit, when diffusion is very fast compared to the reaction processes, we expect the mean-field continuum equation to be valid as has been shown exactly for the process $A \to 2A$ in 1D [9]. In this limit we observe that $V \propto \epsilon_t^{1/2}$, indicating mean-field-like behavior. The agreement with numerical results indeed improves as $\epsilon_t/D \to 0$ [Fig. 3(b)].

IV. FRONT DIFFUSION COEFFICIENT

In order to further study the effects of temporal correlations on the front dynamics, in Fig. 4 we present three sets of results for the front diffusion coefficient. One is the value of D_0 using the approximate value of ρ_1 calculated using the fixed site representation approximation with $l = 2$ in Eq. (9). Another is the value of D_0 calculated with values of ρ_1 obtained from simulations. The third is the value D_f obtained from simulation results. The following observations are immediately evident: (1) For $D = \epsilon_t$, the analytical value D_0 calculated with either ρ_1 agrees well with the simulation result $D_f^{\rm sim}$; (2) for $\epsilon_t > D$, $D_f^{\rm sim} > D_0$; and (3) for $\epsilon_t < D$, $D_f^{\rm sim} < D_0$. These overestimates and underestimates are presumably due to the neglect of the second line of Eq. (8) in the calculation of D_0.

The effect of temporal correlations in the velocity on the front diffusion coefficient that have been omitted in D_0 can be studied using the Green-Kubo result for the asymptotic front diffusion coefficient,

$$D_f = D_0 + \int_0^\infty C(t)dt. \tag{10}$$

Here $C(t)$ is the temporal velocity correlation function defined as

$$C(t) = \langle v(0)v(t)\rangle - \langle v(0)\rangle\langle v(t)\rangle, \tag{11}$$

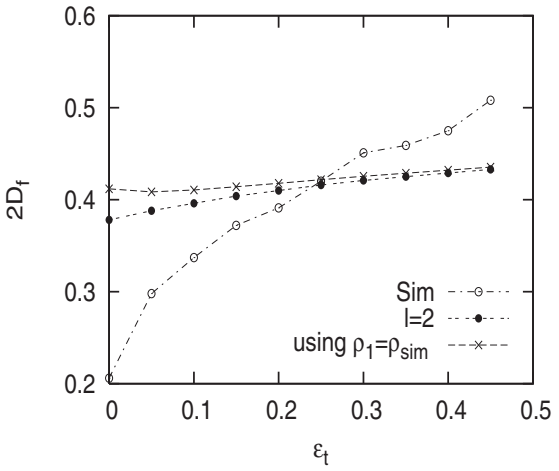

FIG. 4. Comparison of the front diffusion coefficient vs ϵ_t obtained in three ways. The filled circles show D_0 of Eq. (9) with ρ_1 obtained using the approximate value of ρ_1 from the fixed site representation with $l = 2$. The stars show D_0 of Eq. (9) with ρ_1 obtained directly from the simulations. The exact simulation results for D_f are indicated by open circles. Other parameters: $D = 0.25$, $\epsilon = 0.025$. We note that when $\epsilon_t = D = 0.25$, the analytic results exactly match the simulation.

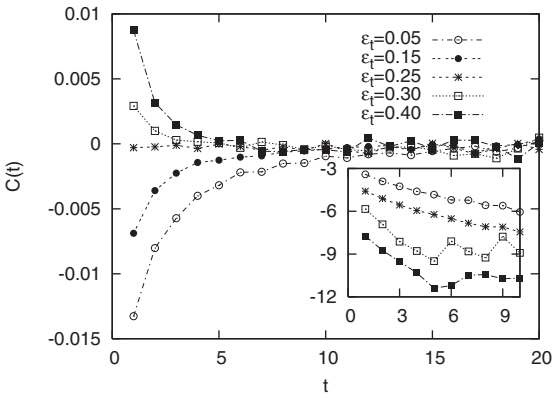

FIG. 5. Simulation results for the time dependence of the velocity correlation of the front for different values of ϵ_t, with $D = 0.25$ and $\epsilon = 0.025$. The velocity correlation is seen to vanish when $\epsilon_t = D$. Inset: Semilog plot of $C(t)$ vs t for $D = 0.05, 0.10, 0.30, 0.40$ from top to bottom.

where $v(t)$ is the displacement of the front per unit time at time t. In Fig. 5 we have plotted the temporal velocity correlations $C(t)$ for different values of ϵ_t. For $\epsilon_t > D$, we observe positive correlations while for $\epsilon_t < D$, the correlations are negative. Most interestingly, for $\epsilon_t = D$, $C(t)$ vanishes for all t. Thus, $\epsilon_t = D$ is a special case for which the front particle moves as an uncorrelated random walker.

We proceed to show explicitly that for the special case $\epsilon_t = D$ two consecutive steps of the leading particle are indeed uncorrelated in the steady state. The analysis is based on the fact that in two successive steps, separated by L microsteps, the front is picked on average once.

Since at most two sites behind the front can be affected in two consecutive steps, we explicitly consider four states corresponding to $l = 2$, namely, {001}, {011}, {101}, and {111}, with the rightmost "1" representing the front. We then write

$$\langle v(t)v(t+1)\rangle = R_{++} - R_{+-} - R_{-+} + R_{--}, \tag{12}$$

where

$$R_{ij} = R_{ij}^{001} + R_{ij}^{011} + R_{ij}^{101} + R_{ij}^{111} \tag{13}$$

denotes the steady-state flux for taking two consecutive steps labeled by $i = \pm$ and $j = \pm$. For example, R_{--}^{001} is the flux of two consecutive negative steps starting from the state 001. The only way this can occur is if the front particle makes two diffusive moves to the left, which in turn can only happen if those sites are empty. Thus $R_{--}^{001} = D^2 P_{001}$, where P_{001} is the steady-state weight of the configuration {001}. Considering all such two successive moves in the each state, we can clearly write

$$\begin{aligned} R_{++} &= D^2 + 2\epsilon D + \epsilon_t D + \epsilon^2 + (\epsilon_t D + \epsilon_t \epsilon)\{P_{001} + P_{101}\}, \\ R_{+-} &= D^2, \\ R_{-+} &= (D^2 + D\epsilon + D\epsilon_t)P_{001} + (D^2 + D\epsilon)P_{101}, \\ R_{--} &= D^2 P_{001}. \end{aligned} \tag{14}$$

This in turn immediately allows us to write

$$\begin{aligned} \langle v(t)v(t+1)\rangle = \epsilon^2 + D\epsilon_t + 2\epsilon D + \{\epsilon_t D + \epsilon_t \epsilon \\ - D^2 - D\epsilon)\}P_{101} + \{\epsilon_t \epsilon - D\epsilon\}P_{001}. \end{aligned} \tag{15}$$

Similarly,

$$\begin{aligned} \langle v(t)\rangle &= \langle v(t+1)\rangle \\ &= \epsilon + \epsilon_t - \{P_{011} + P_{111}\}(\epsilon_t - D). \end{aligned} \tag{16}$$

To compute these quantities we next need to determine the probabilities of the different states that appear in the above expressions. This is in general difficult to do analytically. However, we straightforwardly observe that when $\epsilon_t = D$, the correlation function $\langle v(t)v(t+1)\rangle - \langle v(t)\rangle\langle v(t+1)\rangle$ is independent of all the probabilities and vanishes identically. Thus, two successive steps are temporally uncorrelated, as observed in the simulations, cf. Fig. 5. We also stress that for this special case the above analysis does not involve any approximation, that is, it is exact. This is an interesting nonequilibrium state in which there are spatial correlations but no temporal correlations [22].

When we depart from this special case, it is evident that for $\epsilon_t \neq D$, $\langle v(t)v(t+1)\rangle \neq \langle v(t)\rangle\langle v(t+1)\rangle$, i.e., the front motion is now correlated. Preliminary fits suggest that the temporal velocity correlation function has the general form $C(t) \sim t^{\alpha} e^{-\beta t/\tau}$.

The reaction-diffusion system presented above can be generalized by allowing annihilation of particles, e.g., $2A \to A$ with, say, rate W. The speed of the front in this case may be written following the steps leading to Eq. (7), and we obtain

$$V = \epsilon + \epsilon_t - \rho_1(\epsilon_t + W - D). \tag{17}$$

This implies that for $\epsilon_t + W = D$, the front speed is independent of ρ_1. For this special case the temporal correlations in velocity are also found to vanish numerically. Following the steps used earlier in this section we can explicitly show that two successive steps are indeed uncorrelated. Note that this condition generalizes two special cases. One is the result that we have discussed in this paper, for which $W = 0$ and $\epsilon_t = D$. The other is the well-studied process $A \leftrightarrow 2A$ (no creation of twins, $\epsilon_t = 0$), for which there are no temporal correlations when $W = D$. In Fig. 6 we schematically show the general result, that is, that everywhere on the $\epsilon_t + W = D$ plane the temporal velocity correlations vanish. Furthermore, spatial correlations also vanish on the line $\epsilon_t = 0$, $W = D$. The signs of the temporal correlations (found numerically) are shown in different sections of the coordinate plane. It is interesting to note that for $\epsilon_t > D$, $W = 0$, the sign of the correlations is positive, whereas it is negative on the $D = 0$ and $\epsilon_t = 0$ planes. Thus, if parameters are continuously changed to connect a point on the $\epsilon_t > D$, $W = 0$ plane to one on either of the $D = 0$ or $\epsilon_t = 0$ planes, $C(t)$ must vanish at some intermediate point. This has in fact been verified by our simulation results, as shown in Fig. 7.

V. CONCLUSION

We have studied the front dynamics for the reaction-diffusion system $\{A \xrightarrow{\epsilon} 2A, A \xrightarrow{\epsilon_t} 3A\}$ on a one-dimensional (1D) lattice. We also briefly considered a generalization of this rate scheme in which there is a reverse reaction $2A \xrightarrow{W} A$ whereby an A particle can die. The A particles can random walk onto neighboring sites with transition rate D. No more than one particle may occupy a lattice site, so all of these rate

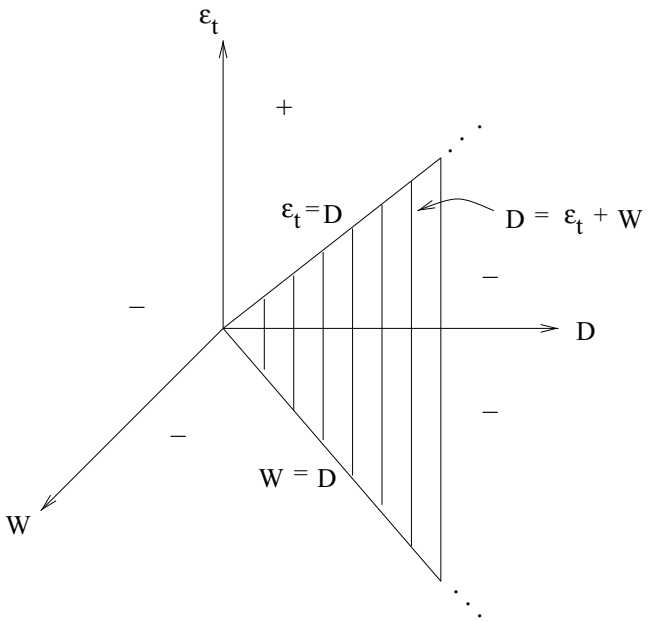

FIG. 6. Schematic representation of the temporal velocity correlation function $C(t)$ for different values of D, W, and ϵ_t, with + and − denoting the sign of $C(t)$. The plane $D = \epsilon_t + W$ corresponds to $C(t) = 0$, which also contains the lines $\epsilon_t = D$, $W = 0$, and $W = D, \epsilon_t = 0$.

processes are only allowed when there are appropriate empty sites to accept the process, be it a singlet birth, a twin birth, or a diffusive step. The rightmost occupied site is defined as the front.

We have calculated the front velocity analytically using different approximate methods. In the fixed site representation one can systematically improve upon estimates of the front velocity by studying the explicit evolution of particles at increasingly larger numbers of sites behind the front. The results from the two-particle fixed site representation procedure and from the mixed representation procedure show gratifying agreement with the simulation results. The mixed representation scheme leads to the simplest generalization of the two-site representation method and can be applied to other processes as well. We also observe that when diffusion is very large compared to the reaction rates, the front velocity converges to the mean-field velocity.

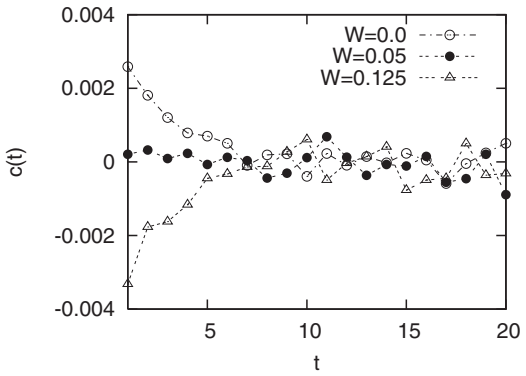

FIG. 7. Simulation results for velocity correlation function of the front as a function of time t, for different values of W while keeping $D = 0.05$, $\epsilon = 0.025$, and $\epsilon_t = 0.15$ fixed. We note that when $W \simeq 0.05$, this correlation is zero.

We have also directed our attention to the front diffusion coefficient. In general, in nonequilibrium interacting systems the temporal velocity correlations affect the diffusion coefficient. However, interestingly, on the parameter plane $\epsilon_t + W = D$ these temporal correlations vanish and the front performs a temporally uncorrelated random walk, a result that we are able to obtain analytically as well as numerically. Furthermore, there are spatial correlations that only vanish when $W = D, \epsilon_t = 0$. This result generalizes one found earlier for the single-particle creation problem $A \leftrightarrow 2A$ [21].

VI. ACKNOWLEDGMENT

Partial support of this work from the NSF under Grant No. PHY-0855471 is gratefully acknowledged.

APPENDIX A: FIXED SITE REPRESENTATION

In this Appendix we illustrate the fixed site representation scheme for the simplest case, $l = 1$. Transitions occur between the two states $\{01\}$ and $\{11\}$ due to the microscopic processes in the system shown in Fig. 8. Considering all such transitions, the probabilities of these two states follow the evolution equations

$$\begin{aligned}\frac{\partial P_{01}}{\partial t} &= (2D - D\rho_2)P_{11} - \{2D\rho_2 + \epsilon(2 + \rho_2) \\ &\quad + \epsilon_t[1 + \rho_2(1 - \rho_3)]\}P_{01}, \\ \frac{\partial P_{11}}{\partial t} &= \{2D\rho_2 + \epsilon(2 + \rho_2) + \epsilon_t[1 + \rho_2(1 - \rho_3)]\}P_{01} \\ &\quad - (2D - D\rho_2)P_{11}. \end{aligned} \tag{A1}$$

Here, ρ_i is the density at the ith site behind the front, and we have neglected the spatial density correlation between consecutive pairs of sites beyond the second site behind the front. Using Eq. (A1) and the normalization condition $P_{01} + P_{11} = 1$, in the steady state we obtain the following

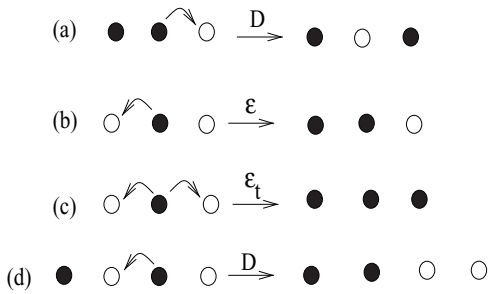

FIG. 8. Microscopic moves. The rightmost • represents the front. (a) Diffusion of the front particle to its right site leading to a transition from $\{11\}$ to $\{01\}$ with a rate D. (b) Creation of one particle to the left of the front leads to a transition from $\{01\}$ to $\{11\}$ with a rate ϵ. (c) $\{01\}$ changes to $\{11\}$ due to the creation of twins at both neighboring sites of the front with a rate ϵ_t. (d) If the front moves diffusively to its left and the second site behind the front is occupied, there is a transition from $\{01\}$ to $\{11\}$ with a rate $D\rho_2$, where ρ_2 is the occupancy probability of the second site behind the front.

expression for ρ_1:

$$\rho_1 = \frac{2D\rho_2 + \epsilon(2+\rho_2) + \epsilon_t[1+\rho_2(1-\rho_3)]}{D\rho_2 + 2D + 2\epsilon + \epsilon\rho_2 + \epsilon_t[1+\rho_2(1-\rho_3)]}. \quad \text{(A2)}$$

In order to find ρ_1 we need to know ρ_2 and ρ_3. As a first approximation we assume that $\rho_2 = \rho_3 = 1$, the bulk density. We then find

$$\rho_1 \simeq \frac{2D + 3\epsilon + \epsilon_t}{3D + 3\epsilon + \epsilon_t}. \quad \text{(A3)}$$

Using this value of ρ_1 in Eq. (7) allows analytic estimates of the front velocity. We can also extend the above procedure to higher values of l.

APPENDIX B: TWO-PARTICLE REPRESENTATION

In this Appendix we use Kerstein's two-particle representation [10,11] for the analytic estimates of the front velocity. We denote by P_k the probability of a two-particle state with k empty sites between the leading particle and the next particle behind it. These states form a closed set under transitions due to microscopic processes. We have illustrated a few transitions in Fig. 9. Considering all such transitions and denoting the probability of occupancy of the site just behind the second particle by ρ, we write the following rate equations for P_k:

$$\begin{aligned}
\frac{\partial P_0}{\partial t} &= (\epsilon + 2D)P_1 + \epsilon_t(1-\rho)P_1 + (2\epsilon + \epsilon_t)(1 - P_0) \\
&\quad - (2D - D\rho)P_0, \\
\frac{\partial P_k}{\partial t} &= (2D - D\rho)P_{k-1} + \{\epsilon + 2D + \epsilon_t(1-\rho)\}P_{k+1} \\
&\quad - (4D - D\rho + 3\epsilon + 2\epsilon_t - \epsilon_t\rho)P_k, \quad k \geqslant 1.
\end{aligned} \quad \text{(B1)}$$

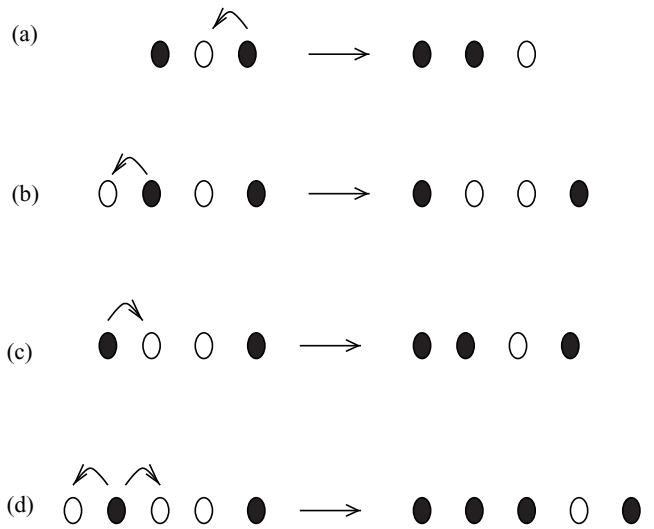

FIG. 9. Transition between two particle states with rightmost • representing front. (a) Diffusive move of the front particle to its left leading to transition $101 \to 11$ with a rate D. (b) When the second particle behind the front jumps to the left, provided it is empty, the state changes from $101 \to 1001$ with a rate $D(1-\rho)$. (c) Birth of a single particle by the second particle to its left with rate ϵ leads to the transition $1001 \to 101$ and (d) $1001 \to 101$ if the second particle gives birth of two particles, provided the site left to it is empty, with a rate $\epsilon_t(1-\rho)$.

In order to solve Eq. (B1) we need to specify the dependence of ρ on the parameters ϵ, ϵ_t, and D. Following Kerstein [11], we write ρ as a linear combination of P_0 and P_0^2 with coefficients to be determined. Enforcing the condition that $\rho = 1$ when $P_0 = 1$ leaves us with a relation in terms of a single free parameter λ,

$$\rho = (1+\lambda)P_0 - \lambda P_0^2. \quad \text{(B2)}$$

This equation implicitly specifies the dependence of ρ on the model parameters through the parameter dependence of P_0. To reduce the infinite set of coupled (linear) equations to a single (nonlinear) equation, we further follow Kerstein and use the ansatz $P_k = P_0(1-P_0)^k$. With Eq. (B2) in Eq. (B1), in the steady state this yields a quartic equation for P_0,

$$\begin{aligned}
&\epsilon_t\lambda P_0^4 + (D\lambda - \epsilon_t - 2\epsilon_t\lambda)P_0^3 + (\epsilon + D + 2\epsilon_t + \epsilon_t\lambda \\
&\qquad - D\lambda)P_0^2 + \epsilon P_0 - 2\epsilon - \epsilon_t = 0.
\end{aligned} \quad \text{(B3)}$$

In order to find P_0 we still need to fix the value of λ. For large D and $\epsilon_t = 0$, it is exactly known that the front particle moves with its mean-field velocity [9]. We have also ascertained this feature numerically for $\epsilon_t \neq 0$ [cf. Fig. 3(b)]. Equating the mean-field front velocity $V_0 = 2\sqrt{(2\epsilon + \epsilon_t)D}$ to that obtained from Eq. (7), i.e., $V \sim DP_0$, for D very large compared to other parameters, we find $P_0 = 2\sqrt{(2\epsilon + \epsilon_t)/D}$. Using this value of P_0 in Eq. (B3), we find $\lambda = 3/4$ in the limit $D \to \infty$. Finally, we solve the quartic equation (B3) to get the value of $\rho_1 = P_0$ and hence the front velocity.

APPENDIX C: MIXED REPRESENTATION

Here we discuss the proposed mixed representation scheme and study the evolution of states {011}, {111}, {0101}, {1101}, ... We denote the states as $(k,0)$ or $(k,1)$, representing the states having k empty sites between the front and the second particle followed by either an empty site or an occupied site, respectively, after the second particle. For example, (0,0) represents the state {011} while (0,1) denotes the state {111}. Some of the transitions in this representation are shown in Fig. 10.

Next, we assume ρ to be the density of the site which is the next nearest neighbor to the second particle. This allows us to write the following rate equation for the evolution of the probabilities $P(k,0)$ and $P(k,1)$, $k = 0,1,\ldots,\infty$:

$$\begin{aligned}
\frac{\partial P(0,1)}{\partial t} &= \{D\rho + \epsilon\rho + 2\epsilon + \epsilon_t\rho(1-\rho)\}P(0,0) \\
&\quad + (D + 2\epsilon + \epsilon_t)P(1,1) + (2\epsilon + 2\epsilon_t)P(1,0) \\
&\quad + \epsilon_t\{P(2,0) + P(2,1) + P(3,0) + P(3,1) + \cdots\} \\
&\quad - (2D - D\rho)P(0,1), \\
\frac{\partial P(0,0)}{\partial t} &= D(1-\rho)P(0,1) + (D+\epsilon)P(1,1) \\
&\quad + (2D + \epsilon)P(1,0) + 2\epsilon\{P(2,1) + P(2,0) \\
&\quad + P(3,0) + P(3,1) + \cdots\} - \{2D + 2\epsilon + D\rho \\
&\quad + \epsilon\rho + \epsilon_t\rho(1-\rho)\}P(0,0), \\
\frac{\partial P(k,1)}{\partial t} &= DP(k-1,1) + D\rho P(k-1,0) \\
&\quad + \{D\rho + \epsilon + \epsilon\rho + \epsilon_t\rho(1-\rho)\}P(k,0)
\end{aligned}$$

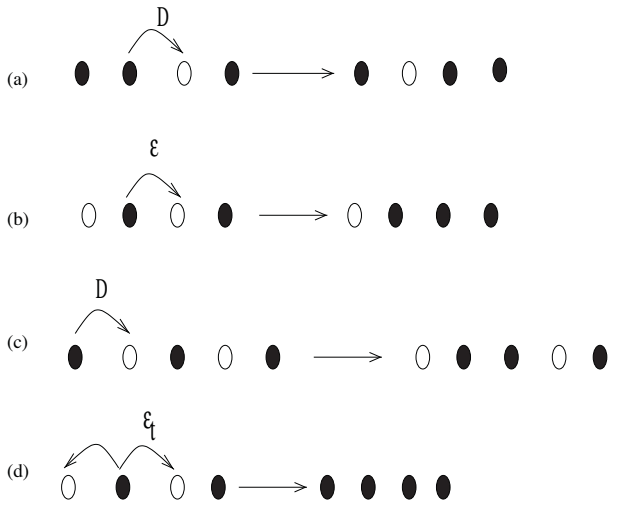

FIG. 10. Transitions between mixed particle states with the rightmost • representing the front. (a) Diffusive move of the particle to the right empty site with a rate D. This leads to a transition from (1,1) to (0,0). (b) Birth of a new particle on the right neighboring empty site with a rate ϵ, which changes the state (1,0) to (0,1). (c) Transition from (1,0) to (1,1) with a rate $D\rho$, when the third particle jumps to the right neighboring empty site. (d) (1,0) $\rightarrow$ (0,1) when the second particle behind the front in (1,0) produces twins at the neighboring empty sites with a rate ϵ_t.

$$\begin{aligned}
&+(D+\epsilon)P(k+1,1)+(\epsilon+\epsilon_t)P(k+1,0)\\
&-(4D+3\epsilon-D\rho+\epsilon_t)P(k,1),\\
\frac{\partial P(k,0)}{\partial t} &= [D+D(1-\rho)]P(k-1,0)+D(1-\rho)P(k,1)\\
&+DP(k+1,1)+2DP(k+1,0)-\{4D+4\epsilon\\
&+D\rho+\epsilon\rho+2\epsilon_t+\epsilon_t\rho(1-\rho)\}P(k,0). \qquad \text{(C1)}
\end{aligned}$$

This is an infinite set of (linear) coupled equations. We truncate the problem and find an analytic estimate for P_0 by solving the rate equations for $P(0,0)$ and $P(0,1)$, assuming $P(1,1)=\rho P_1$, $P(1,0)=(1-\rho)P_1$. Using $\sum_{i=0}^{1}P(k,i)=P_k$ and $\sum_{k=0}^{\infty}P_k=1$, we find the steady-state expression for $P(0,0)$ and $P(0,1)$ in terms of P_1 and ρ, which in turn leads to an expression for P_0 in terms of these quantities since

$$P(0,0)+P(0,1)=P_0. \qquad \text{(C2)}$$

Following Kerstein [11], we use the ansatz $P_1=P_0(1-P_0)$ and arrive at the equation

$$\alpha P_0(1-P_0)+\beta P_0+\gamma=0, \qquad \text{(C3)}$$

where

$$\begin{aligned}
\alpha &= (2\epsilon+\epsilon_t+D\rho-\epsilon_t\rho)\{3D+2\epsilon+\epsilon\rho+\epsilon_t\rho(1-\rho)\}\\
&\quad+(2D-D\rho-\epsilon)\{2D+2\epsilon+\epsilon\rho+\epsilon_t\rho(1-\rho)\},\\
\beta &= \{2D+2\epsilon+\epsilon\rho+D\rho+\epsilon_t\rho(1-\rho)\}(2D-D\rho)\\
&\quad-\{D\rho+2\epsilon+\epsilon\rho+\epsilon_t\rho(1-\rho)\}(D-D\rho),\\
\gamma &= \epsilon_t(1-P_0)\{3D+2\epsilon+\epsilon\rho+\epsilon_t\rho(1-\rho)\}\\
&\quad+2\epsilon(1-P_0)\{2D+2\epsilon+\epsilon\rho+\epsilon_t\rho(1-\rho)\}. \qquad \text{(C4)}
\end{aligned}$$

Equation (C3) contains the two unknowns ρ and P_0. We therefore need an additional relation between them to find the desired P_0. We specify the dependence of ρ on P_0 in a way analogous to the procedure followed in the case of the two-particle representation (see Appendix B), and thereby arrive at analytic estimates for P_0 and hence for the front velocity. The expressions are rather cumbersome and so we only exhibit the results graphically in Fig. 1.

[1] W. van Saarloos, Phys. Rep. **386**, 29 (2003).

[2] M. G. Clerc, D. Escaff, and V. M. Kenkre, Phys. Rev. E **72**, 056217 (2005).

[3] M. A. Fuentes, M. N. Kuperman, and P. De Kepper, J. Phys. Chem. A **105**, 6769 (2001).

[4] G. Abramson, V. M. Kenkre, T. L. Yates, and R. R. Parmenter, Bull. Math. Biol. **65**, 519 (2003).

[5] In interacting systems the diffusion coefficient is a function of the mean density. In the limit of very low mean densities Γ approaches the bare diffusion constant of the particles. In this model the bulk density is 1 and hence the mean-field computation of the front speed is valid only for *pulled* fronts for which the dynamics is set at the leading edge where the mean density approaches zero. This issue is of not much concern to us as we compute the speed from the microscopic model directly.

[6] R. A. Fisher, Ann. Eugenics **7**, 355 (1937); A. Kolmogorov, I. Petrovsky, and N. Piscounov, Moscow Univ. Bull. Math. A **1**, 1 (1937).

[7] Niraj Kumar and G. Tripathy, Phys. Rev. E **74**, 011109 (2006).

[8] Niraj Kumar and G. Tripathy, Phys. Rev. E **75**, 021117 (2007).

[9] M. Bramson, P. Calderoni, A. De Masi, P. A. Ferrari, J. L. Lebowitz, and R. H. Schonmann, J. Stat. Phys. **45**, 905 (1986).

[10] A. R. Kerstein, J. Stat. Phys. **45**, 921 (1986).

[11] A. R. Kerstein, J. Stat. Phys. **53**, 703 (1988).

[12] K. Krebs, F. H. Jafarpour, and G. M. Schütz, New J. Phys. **5**, 145 (2003).

[13] S. Redner, in *Nonequilibrium Statistical Mechanics in One Dimension*, edited by V. Privman (Cambridge University Press, Cambridge, U.K., 1997).

[14] E. Brunet and B. Derrida, Phys. Rev. E **56**, 2597 (1997); J. Stat. Phys. **103**, 269 (2001).

[15] V. Kuzovkov and E. Kotomin, Rep. Prog. Phys. **51**, 1497 (1988); E. A. Kotomin and V. N. Kuzovkov, *Modern Aspects of Diffusion-Controlled Reactions* (Elsevier, Amsterdam, 1996).

[16] J. Mai, I. M. Sokolov, and A. Blumen, Phys. Rev. Lett. **77**, 4462 (1996); J. Mai, I. M. Sokolov, V. N. Kuzovkov, and A. Blumen, Phys. Rev. E **56**, 4130 (1997).

[17] N. G. van Kampen, *Stochastic Processes in Physics and Chemistry* (North-Holland, Amsterdam, 1981).
[18] D. Panja, G. Tripathy, and W. van Saarloos, Phys. Rev. E **67**, 046206 (2003).
[19] D. Panja, Phys. Rep. **393**, 87 (2004).
[20] B. D. Hughes, *Random Walks and Random Environments* (Oxford Science, New York, 1995).
[21] D. ben-Avraham, Phys. Lett. A **247**, 53 (1998).
[22] In many nonequlibrium steady states of interacting driven lattice models with product measure, e.g., asymmetric simple exclusion process on a ring, spatial density correlations vanish in the steady state whereas there are nontrivial temporal correlations in velocities. See, e.g., G. M. Schütz, *Phase Transitions and Critical Phenomena*, Vol. 19 (Academic, London, 2000).